Extreme call amplitude from near field acoustic wave coupling in the stridulating water insect *Micronecta scholtzi* (Micronectinae)

Andrew Reid[1], David J W Hardie[2], David Mackie[1], Joseph C. Jackson[1], James F.C. Windmill[1]

[1]University of Strathclyde, Centre for Ultrasonic Engineering, Department of Electronic & Electrical Engineering, Glasgow G1 1XW, United Kingdom.
[2]Thales Maritime Mission Systems, Templecombe, Somerset BA8 0DH, United Kingdom.

November 24, 2017

Abstract

Underwater acoustic transducers, particularly at low frequencies, are beset by problems of scale and inefficiency due to the large wavelengths of sound in water. In insect mating calls a high call volume is usually desirable, increasing the range of signal transmission and providing a form of advertisement of the signaller's quality to a potential mate, however the strength of the call is constrained by body size as well as by the need to avoid predators who may be listening in. Male crickets and water boatmen avoid some of the limitations of body size by exploiting resonant structures, which produce sharply tuned species specific songs but call frequency and volume remain linked to body size. Recently the water boatman *Micronecta scholtzi* was found to circumvent this rule, producing a louder mating call than similar, but much larger *Corixa*. The resonant structure in *Corixidae* and *Micronectinae* is believed to be the trapped air reserves around the insect as it dives, driven by a stridulatory apparatus. However, the method by which energy is transferred from striated area to bubble is unknown. Here we present modelling of a system of near-field coupling of acoustic sources to bubbles showing an exponential increase in sound power gain with decreasing distance that provides a simple solution to the stimulus of the air bubbles in *Corixida* and *Micronectinae* and explains the discrepancy of *Micronecta scholtzi*'s extreme call volume. The findings suggest a possible route to engineered systems using near-field coupling to overcome size constraints in low-frequency ($< 500Hz$) underwater transducers, where the input efficiency of a piezoelectric device can be coupled through the hydrodynamic field to the high radiative efficiency of a near ideal monopole emitter.

Keywords

Micronecta scholtzi, underwater acoustics, near-field acoustic coupling, water boatmen.

Introduction

Micronectinae are an extremely widespread and populous subfamily of Corixidae of the sub order Hydrocorisae, yet despite their near worldwide distribution studies on the family are sparse. From the remaining two clades, *Corixinae* and *Diaprepocorinae*, the *Corixidae* have extensive morphological and physiological studies, while investigations into *Micronectinae* are frustrated by their small size (1.5-6.0 mm) [1] and *Diprepocinae* consists of a single rare genus

which occurs only in Australia and New Zealand. Recently *Micronecta scholtzi*, a common aquatic heteroptera, was identified as having an extremely loud mating call in relation to its body size, reaching a peak of 99.2 dB SPL (ref 20 μPa, air equivalent level) at a distance of one metre [2]. The average body length of *M. scholtzi* is not more than 2.5 mm in length, therefore the emission of such an intense signal seems to contradict the expected correlation between body size and call amplitude [3].

In common with *Corixinae* the mechanism of sound production is believed to be stridulation, although the site of the plectrum and file (*pars stridens*) appears significantly different. In *Corxidae* striated areas and the plectrum are located on the fore femora and the head capsule respectively [4] while in *Mictronecta batilla* and *Micronecta scholtzi* the *pars stridens* appears to be located on the posterior abdominal segment [5]. A striated area is observed in *Micronecta gracilis*, *Micronecta australiensis* and *Micronecta batille* [6] on the right side of the 6th tergite and in *Micronecta scholtzi* on the right paramere of the genital appendage [7], however no direct observation of stridulation has been achieved. The *pars stridens* in *M. scholtzi* is particularly small at only 50 μm in length, compared to 100 μm in *M. batilla*. Males of all species produce a distinct song which is species specific [8]. The song is produced only by the males and takes the form of a pulse train with two or three echemes, which is obligatory for copulation to be successful [**?**]. Males appear to be able to synchronize their calls generating a chorus [8].

Production of high amplitude mating calls may be facilitated by exploiting structural resonance for sound radiation, such as the wing in *Gryllus bimaculatus* [9]. In corixids the resonant structure is provided by the air cushion maintained by the diving insect as an air reserve, evidenced by the strong correlation between the calling frequency of the animal and the air volume in the reserve [10]. Air cushions in submerged Corixids are distributed over the ventral surface, maintained by hydrophobic hair structures and on the dorsal surface of the abdomen and between the abdomen and the elytrum [11]. These air cushions make ideal resonators, producing a pure tone at the Minnaert frequency which scales inversely with the square root of the bubble volume [12]. The recorded calls of *C. dentipes*, *C. punctata* and *Micronecta scholtzi* all are found to be pure tones [10, 2], and in the case of the Corixids were found to not only decrease in frequency with body size but also increase over the length of time submerged as the air reserves are depleted [10].

Corixa generate underwater sound by means of volume pulsations of this air cushion, with the mating call of one animal also stimulating the resonant behaviour of the air cushion in nearby animals [10]. Unfortunately the *pars stridens* in the same animal is located on the fore femora, where it would also be enclosed by the ventral air cushion presenting a significant problem for sound transmission due to the large impedance mismatch between the air and water. Neither is the sound power from strigilation in air likely to be strong enough to excite significant volume pulsation in the air cushion. *Micronecta scholtzi*'s plectrum and *pars stridens*, being located below the 5th tergite of the abdomen is more likely to be submerged in water, allowing not only the excitation of the bubble resonance by the more powerful free field in water but due to its extreme proximity to the bubble to excite pulsation through the far higher pressures of the hydrodynamic near field. The transfer of energy from striated area to bubble in the formulation would be extremely efficient, allowing the multi-pole, highly directive sound field produced by a plectrum and comb to drive the far more efficient, near ideal monopole source formed by the air cushion. Here we present analytical models of the pressure gain from the presence of a bubble in the near field of monopole and dipole sources and compare the results with Finite Element Analysis simulations of *M. scholtzi*'s body and air cushions to demonstrate that significant pressure gains can be achieved. It is proposed that the small size of *Micronecta scholtzi*, reducing the separation between plectrum and *pars stridens* and bubble, is responsible for the high call volume and that taking into account the bubble gain the relationship between call volume and sound pressure level falls within the expected range of other stridulating insects.

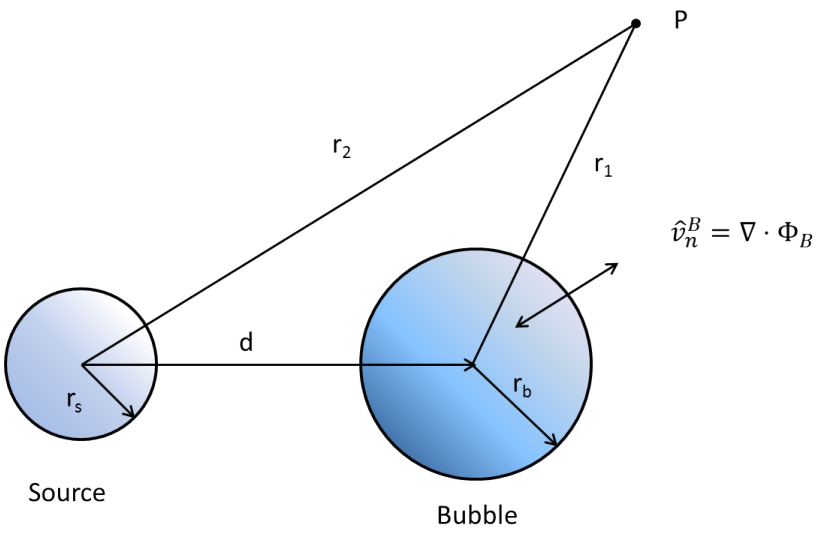

Figure 1: Simplified system of source and bubble. The velocity potentials from the bubble and source taken at two points: at the bubble boundaries (Φ_s^B) and (Φ_b^B) for source and bubble velocity potentials at the bubble wall respectively) and at some listening point P away from both source and bubble (Φ_s^P) and (Φ_b^P). The velocity potential of the incident wave measured at the bubble boundaries (Φ_s^B) is assumed to be uniform around the bubble if the wavenumber $k >> r_b$ (where $k = \frac{\omega}{c}$) and $d >> r_b$.

Theory

The acoustic output of a source can be significantly increased by the presence of nearby scatterers, particularly by resonant cavities. A submerged gas bubble can be thought of as a simple oscillatory system, with the spring represented by the compressed air within the bubble and the mass being that of the water displaced by the movement of the bubble's boundaries. For a simple volume pulsation the natural resonance frequency of a submerged gas bubble is given by Houghton [13] as:

$$\omega_0 = \left[\frac{3\gamma P_W}{\rho r_0^2} + \frac{2\sigma(3\gamma - 1)}{\rho r_0^3} + \frac{4\eta}{\rho^2 r_0^4}\right]^{\frac{1}{2}} \tag{1}$$

where P_W is the hydrostatic water pressure, ρ the water density, r_0 the radius of the bubble and γ the ratio of specific heats in the gas. The second term takes account of the surface tension σ while the third includes the effect of the dynamic viscosity of the liquid η. The first term gives the approximate Minnaert resonant frequency, which can be used to relate the velocity potentials from the source (Φ_s) and bubble (Φ_b) at the bubble wall (here denoted by 'b') (Figure 1) [14]:

$$\Phi_b^B = \Phi_s^B \left[\frac{\omega_0^2}{\omega^2} - 1 - \imath\delta\right]^{-1} \tag{2}$$

where ω_0 is the Minnaert resonance frequency of the bubble while δ is a damping parameter which encompasses radiative, thermal and viscous losses and $\imath$ is the imaginary unit. The Minnaert frequency has little dependence on bubble shape, so air bubbles of similar volume will have the same angular frequency of resonance with small errors [15] and is assumed, in this formulation, to produce sound as a near ideal monopole source. This model was developed to predict behaviour in the far field of a sound source and assumes there will be no dipole motion of the bubble in the absence of a restoring force, however in the near field of a source the relative velocity of the bubble and hydrodynamic flow around the source provides the necessary restoring force for dipole motion. In the near field the sound field scattered from a bubble will

be dominated by the monopole motion of the bubble, but a significant underestimation of the total sound field will be made if the dipole motion is not also considered. The pressure gains are calculated at an arbitrary listening point 'P' as the ratio of the pressure from the bubble acting as a monopole and the incident pressure from the source; the full derivation of the equations for pressure gain of a bubble in the near field of a monopole or dipole source is given in Appendix 1. For monopole gain on a logarithmic scale:

$$A_{dB,monopole} = 20\log_{10}\left|\frac{\frac{r_b}{d}}{\frac{\omega_0^2}{\omega^2} - 1 - \imath\delta}\right| \tag{3}$$

The pressure gain A is given in terms of the bubble radius r_b, distance d between source and bubble, the angular velocity of the source ω and the Minnaert resonance of the bubble ω_0. Thermal and viscous losses are incorporated in the term δ. Similarly for a dipole source the increase in sound pressure as the result of the submerged gas bubble in the near field would be:

$$A_{dB,dipole} = 20\log_{10}\left|\frac{\frac{kd+\imath}{d^2}\cos(\theta_b)\frac{r_b}{r}}{\frac{kr+\imath}{r^2}\cos(\theta_1)\left(\frac{\omega_0^2}{\omega^2} - 1 - \imath\delta\right)}\right| \tag{4}$$

where in addition to the dependence on separation between source and bubble d, bubble radius r_b and angular velocity ω there is a dependence on the angle between source and bubble θ_b and the angle between source and listening point P (θ_1). The distance to the listening point r also appears in this equation although if $kr >> 1$, i.e. the listening point is in the far field, that dependence disappears. Dipole gains are significantly higher than monopole gains in the near field, being inversely proportional to the square of the distance between source and bubble. The presence of the bubble in the near field essentially couples the low transmission efficiency of a multi -pole source to the high transmission efficiency of a near ideal monopole. The equations above consider only the monopole action of the source and so underestimate the pressure gain. Calculation of the dipole motion of the bubble in the near field was provided by Ffowcs-Williams [16], however the solution is complex and difficult to apply to more general cases than ideal sources making finite element analysis a more attractive strategy for determining the complete pressure gain from the bubble as a scatterer. A comparison of the pressure gain estimations from this simple monopole model and FEA analysis is shown in Figure 2.

Method

Micronecta schlotzi used in this work were provided by Dr Jérôme Sueur of Muséum national d'Histoire naturelle, Département Systématique et Evolution and were collected from Paris and Morsang-sur-Orge. The sample *M. scholtzi* were preserved in 70% ethanol, and were unsexed at the time of scanning. X-Ray microscale Computer Tomography (μCT) scans were performed using a Bruker Skyscan 1172. The insect was prepared by removing it from the ethanol and drying for a period of 8 hours, then mounting on a block of dental wax with ventral side up and encasing the insect in a plastic straw. The scans shown here were conducted using a voltage of 50 kV on the X-Ray source, with no filter applied to obtain the maximum contrast between the often uniform X-Ray attenuation coefficients of the insect's soft body. Images were generated with 2664 x 4000 pixels at a resolution of 1.36 μm per pixel, with 4 frame averages taken at each 0.3° increment around one hemisphere of the insect body. 3D volumetric reconstruction was performed using Bruker's CTvol software, and the image resized and noise reduced using the same suite's CTAn program. Six *Micronecta scholtzi* were scanned in this way with the best image of a respresentative male being used to generate a 3D model of the insect body for Finite Element Analysis simulations.
The acoustic scattering problem was simulated in COMSOL Multiphysics version 5.3.1 using a

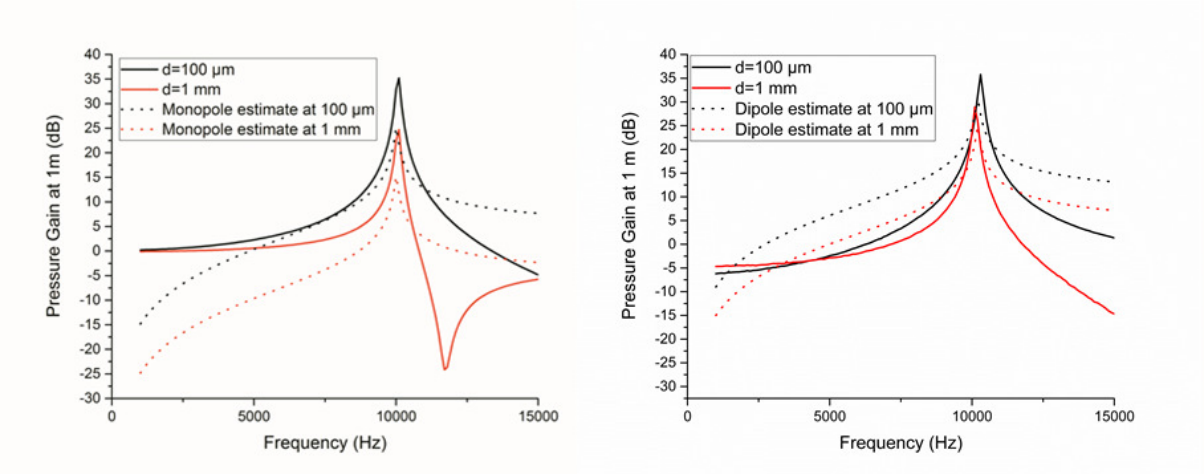

Figure 2: Comparison of pressure gain from bubble in the near field of a source at a distance of 1 meter from the bubble estimated from COMSOL modelling (solid lines) and monopole approximation derived above (dotted lines). (Left) Monopole source at distances of 100 µm and 1 mm. (Right) Dipole source at distances of 100 µm and 1 mm.

3D Pressure Acoustics model of a 326 μm radius air bubble contained within a 20 mm radius spherical water domain, the boundaries of which are modelled as a perfectly matched layer mimicking an infinite water domain. Minimum mesh element size was constrained to 9 μm due to the size of the source and fine detail on the model *M. scholtzi* body while the source frequency was swept in 200 Hz steps from 1 kHz to 20 kHz with a minimum of 543 mesh elements per wavelength at high frequencies. The plectrum and *pars stridens* are located on the last segment of the abdomen, which is split, and the exact nature of the vibrations and resulting sound source are unknown. Here we assume the majority of the bodily vibrations are concentrated on the last segment, and simulate the source as the sound field on a spherical surface of 50 μm radius which encompasses the site of strigilation, treating the boundary as an acoustic hologram which is continuous with the water domain to omit the consideration of backscatter. The insect body itself was modelled as an acoustically rigid boundary (Neumann boundary condition). The locations of the bubbles were taken as being on the ventral side of the insect body omitting the site of stridulation and the head capsule and on the dorsal side underneath the elytrum in line with previous estimates of bubble locations [10]. The bubble dimensions were chosen to obtain a volume that would produce a Minnaert resonance at 10 kHz to match the frequency of the call of *Micronecta scholtzi*.

To simulate the sound field around *M. scholtzi*'s body a model of the insect in a normal swimming posture was required, which was considered in the simplified case here to be a model of the abdomen, thorax and head capsule omitting the legs. Here the coronal cross section images generated by the μCT scans were used, as generating a full body model directly from the floating point mesh of the insect proved too computationally expensive. Slices of *Micronecta scholtzi* were taken every 20 μm along the insect length and traced in series of 67 work planes in Autodesk Inventor generating a wireframe model of the body. The slices were joined via a series of 20 μm thick lofts, and the resulting solid body imported into COMSOL Multiphysics (Figure 3). Two air domains were considered, one on the ventral surface and one on the dorsal surface. The ventral bubble was considered bounded only by ventral surface of the insect body, while the dorsal bubble was treated as being nearly totally enclosed by the insect abdomen and elytrum save for a 100 μm wide belt around the minor axis of the bubble. The attachment to the insect body would be expected to change the resonance frequencies due to the unbalanced hydrodynamic field around the bubbles, resulting in a more damped resonance frequency and allowing a coarser frequency sweep and reduced computation times. The sound source in the

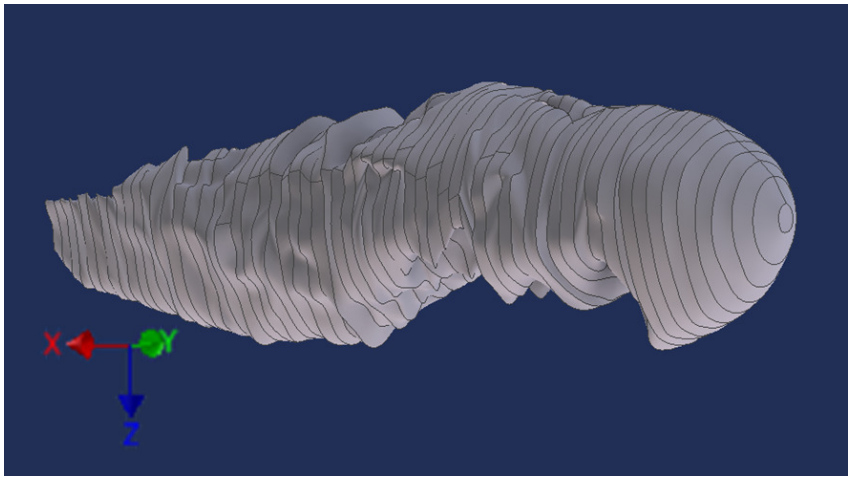

Figure 3: 3D Model of M. scholtzi generated in CAD using a series of 2D slices at 20 μm intervals around the body of the insect (marked by the contour lines along the long axis of the insect). Each slice was connected with a loft and the resultant solid converted to a tetrahedral mesh and imported into COMSOL for use in finite element simulations.

free field was treated as a simple piston with a prescribed acceleration of 0.1 m/s^2 which, in a free field, generated a sound pressure level of 7.35 dB SPL (ref 1 μPa) at the water domain boundaries 30 mm from the centre of the bubble along the axis of maximum amplitude. The source strength was chosen arbitrarily as we are looking for the relative gain with the presence of the bubble in the near field which is expected to be linear with amplitude. Hydrostatic water pressure was taken as 100 kPa, equivalent to 1 m depth.

Results

The volume and location of the air cushions for the COMSOL models were taken from the μCT scans of *M. scholtzi* (Figure 4). The bubble volumes were treated as ellipsoids intersected by the insect body, with the depth and wetting area on the insect body being determined by the resonance frequency. Both the volume underneath the elytrum and that on the ventral surface of the insect resonated at 10 kHz with a wetting area that comprised the entire abdomen in the case of the dorsal bubble and a wetting area that spanned from the head capsule to the lower abdomen in the case of the ventral bubble (Figure 5). Bubble depth in the ventral bubble was 180 μm while the dorsal bubble depth was 150 μm. For a simple dipole source placed at the posterior side of the abdomen at the approximate location of the pars stridens pressure gains of +42.27 dB (in comparison to 7.35 dB free field) could be observed at resonance for the ventral bubble only and +39.41 dB for the dorsal bubble only, the change likely reflecting the increased distance from the simulated stridulation site to the ventral bubble. A compiled list of the scenarios tested and the resulting pressure gains from the presence of the bubble in given in table 1. When both bubbles are present, however, their oscillations become linked by the fluid domain between them and two resonance peaks occur: the first as the bubbles oscillate in phase and the second at higher frequency as the bubbles oscillate out of phase giving a dipole sound field (Figures 7 and 8). It is equally possible to have the two air domains linked around the neck underneath the wing hinges where the system will act as a single bubble however the depth of the air cushion on the ventral surface then decreases significantly. This remains the most likely scenario given the absence of a secondary peak in recordings of *M. scholtzi*'s mating call [2].
In comparisons with the source placed inside the air cushion the resonant peak at 10 kHz was also observed, however the resulting field was still considerably attenuated by this process

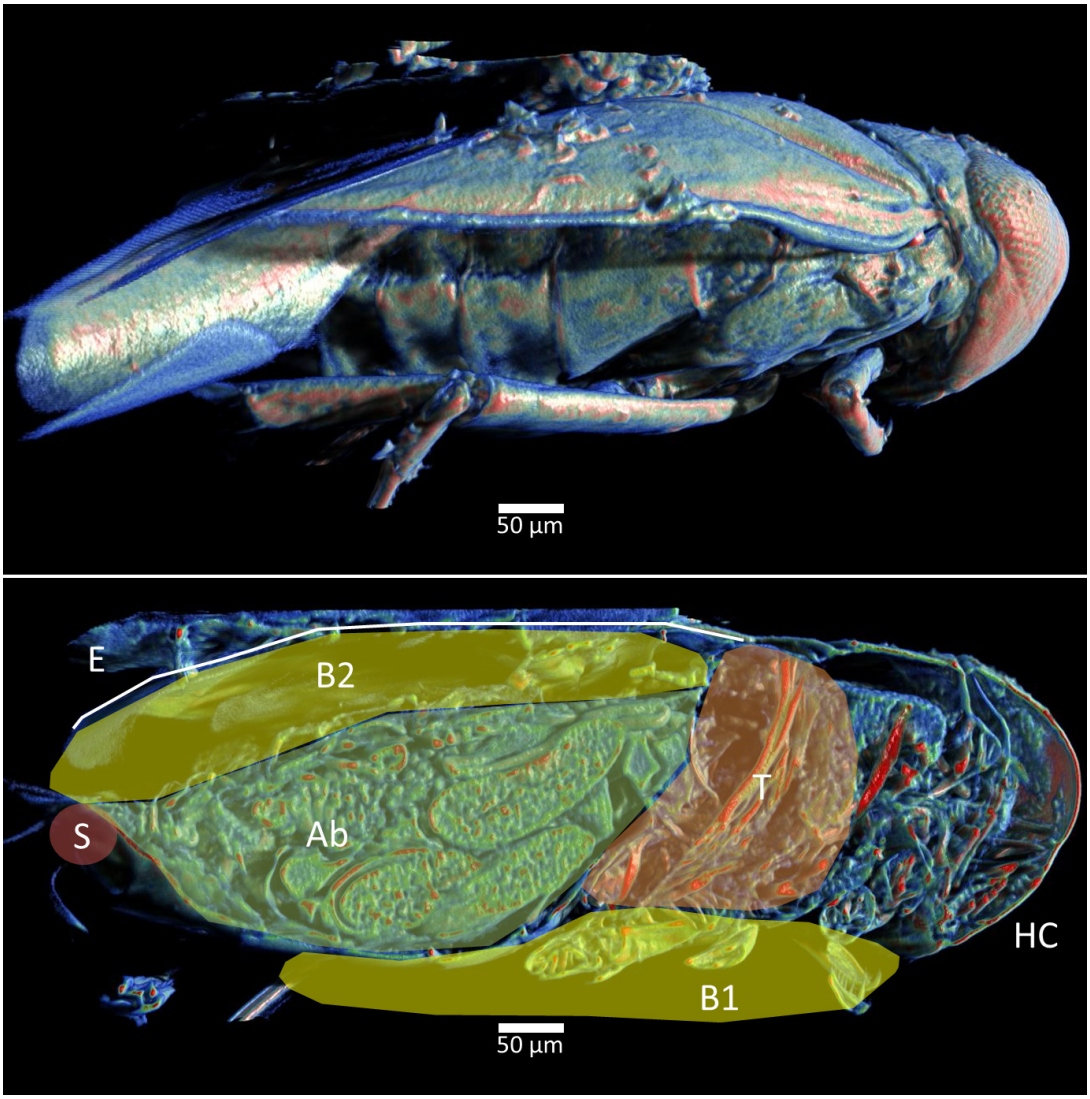

Figure 4: Micro CT images of Micronecta scholtzi. (Top) Sagittal view of entire insect. (Bottom) Cross section sagittal plane annotated with locations of abdomen (Ab), thorax (T), head capsule (HC),elytrum (E) and likely sites of air bubbles (B1, B2) and approximate location of pars stridens (S).

Scenario	SPL at listening point	SPL Gain
Dipole source only	7.35 dB	0
Dipole + Ventral Bubble	49.62 dB	+42.27 dB
Dipole + Dorsal Bubble	46.76 dB	+39.41 dB
Dipole + Linked Bubbles	52.74 dB	+45.39 dB
Dipole + Unlinked Bubbles	33.64 dB (10kHz), 31.28 dB (13.2 kHz)	+26.29 dB, +23.93 dB

Table 1: Pressure gains from finite element simulation scenarios. All scenarios presented here are in relation to a dipole source, although the real sound field is likely to be higher order. For each test the bubble volume was adjusted to produce a Minnaert resonance at 10 kHz, resulting in a thinner layer around the body of M. scholtzi for the scenario in which the bubbles are linked around the body. Where both bubbles are present but not linked (final row) there are two resonance peaks, one in which the bubbles move in phase at 10 kHz and one in which they move in anti-phase with respect to each other at 13.2kHz and the gains for both are presented.

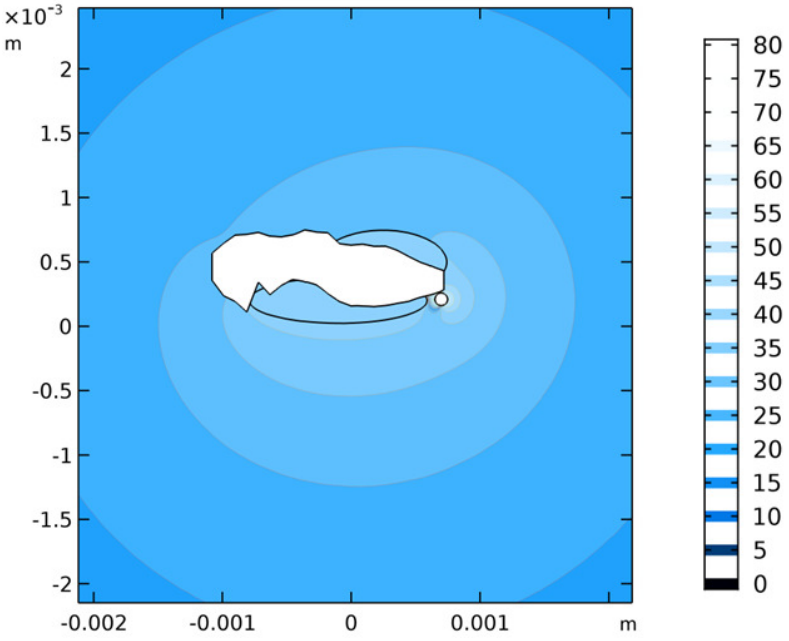

Figure 5: COMSOL image of sound field around Micronecta scholtzi body, showing the air bubbles acting as a monopole source in the far field. Sound pressure level given in dB ref 1 μPa.

reaching a peak pressure gain of -19.76 dB in the case of a monopole source and -10.51 dB in the case of a dipole source. Additional simulations were performed with the *M. scholtzi* body model using a sawtooth waveform stimulus from the source to approximate the clicks of stridulation. The fundamental frequency was set to 5 kHz, 10 kHz and 15 kHz for three total simulations in the time domain which is a considerably larger range than might be expected from temperature variations in plectrum stroke speed. Resonant peaks remained constant at 10 kHz from the bubble resonance with pressure gains from the 5 kHz and 15 kHz sawtooth waves calculated as 75% and 22% of the matched frequency pressure gain at 10 kHz.

Discussion

Previous research on the mating call of aquatic Heteroptera has suggested that the striated area lays within the air cushion, which then acts as a sound box amplifying the signal, however even when stimulated with a signal matched to the natural resonance frequency of the air cushion the signal is considerably attenuated rather than amplified. In the bubble as oscillatory system the mass is provided by the water surrounding the bubble which the relatively small amplitude of pressure variations in air is unable to significantly affect. In the near field of any acoustic source the acoustic impedance is primarily reactive - the force exerted on the medium accelerates rather than compresses it. Energy is not transmitted but merely transferred back and forth in the flow around the source. Perhaps counterintuitively for an acoustic source in the near field we can treat the fluid motion as incompressible, since when the source is small in comparison to the wavelength the transmitted energy is negligible in comparison to the energy of the fluid flow. The bubble placed within this reactive field can then be driven by these much higher hydrodynamic pressures, using the static field to drive a near ideal monopole source. The system might be described as an acoustic analogy of evanescent near-field coupling in electromagnetic waves with the maximum energy transfer occurring when the source frequency matches the bubble resonance [17]. The apparent gains in sound power and sound pressure are the result of the bubble's increased efficiency at generating an acoustic wave in comparison to the source, hence the far greater gains from dipole or higher order sources than those observed with monopole

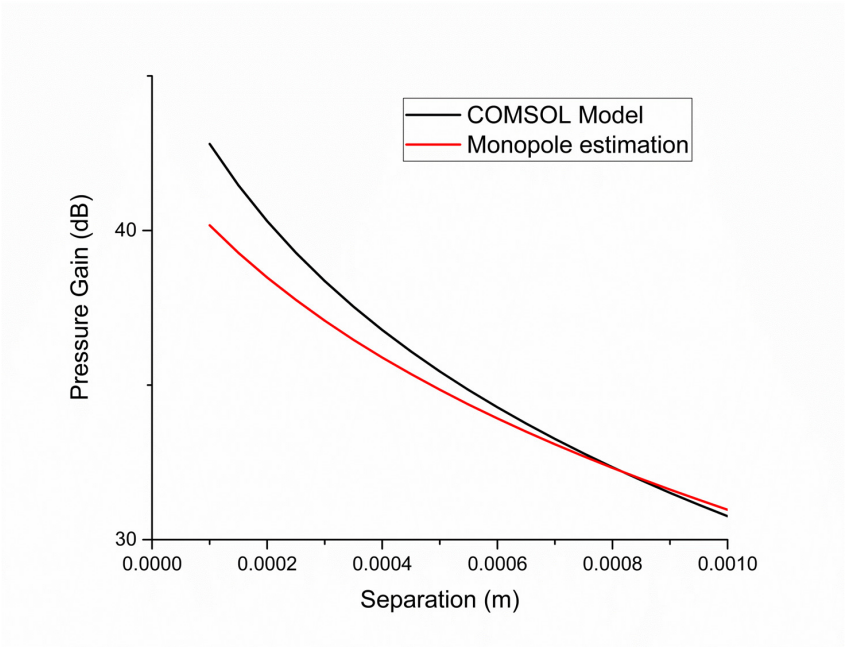

Figure 6: Graph comparing the estimates of pressure gain due to the presence of the bubble with separation between the bubble and source from finite element simulations (COMSOL) and analytic model. The pressure gain is calculated at 30 mm from the ratio of pressure with source and bubble to source only. The analytical model overestimates gain at very small separations compared to finite element modelling.

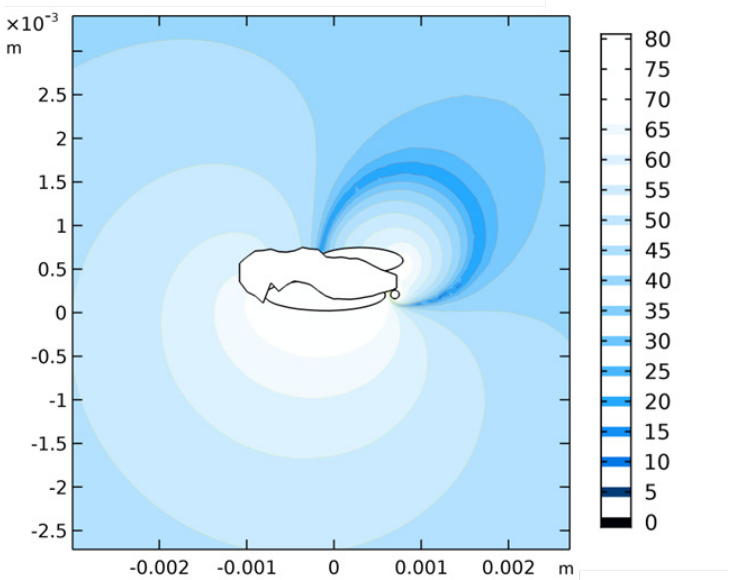

Figure 7: If dorsal and ventral bubbles are separate and of approximately equal volume, the single resonance peak splits and two modes are apparent: a lower frequency monopole where the bubbles oscillate in phase and a higher frequency dipole are the bubbles oscillate in anti-phase. The image above shows the resulting dipole sound field from two bubbles stimulated at 13.2 kHz.

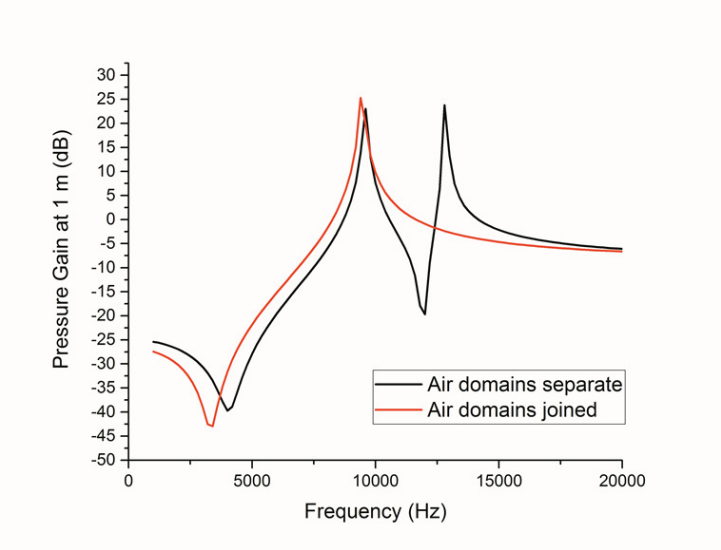

Figure 8: Finite element simulations of single linked bubble showing a single peak (monopole) and separated bubbles with two resonance peaks at 10 kHz (monopole) and 13.2 kHz (dipole). With the dorsal and ventral bubbles linked by any wetted surface a single peak is seen at the resonance frequency of the new bubble volume, here reduced to retain the peak at 10 kHz.

sources. In essence a poor acoustic radiator which is relatively easy to drive is coupled with a very efficient radiator.

The high call volume of *Micronecta scholtzi* song is potentially explained by the inverse relationship between separation between source and bubble and sound power gain. The insects small size and necessary proximity between the striated area and bubble resonator, simulated here as a separation of 120 μm offers a high coupling efficiency. Previous work on *Micronecta scholtzi* [2] has speculated that the volume of the call was an example of runaway selection in the absence of suitable predators, however the model presented here would point to the call volume being caused by the adaptation of an existing mechanism to a smaller body size. The call volume is possibly a by-product of pressures towards a smaller body size rather than sexual selection for higher call amplitude.

Both the ventral and dorsal air cushions have the potential to act as resonators for the mating call; however if both are present as separate bubbles the resulting call would show two resonance peaks since they are essentially being 'rung' be the near-field pressure. Recordings of *M. scholtzi* show only a single peak, suggesting that the air cushions on the ventral and dorsal surfaces are linked. The measurements of *M. scholtzi*'s call volume was given in previous research as reaching a peak of 99.2 dB SPL with reference to 20μ Pa [2]. The figure quoted has been converted to an air equivalent level in order to make a direct comparison to the SPL at 1 m of other animals' mating calls, taking the average of the ratio of SPL (dB)/(3$\times \log_1 0$ body length) to draw ordinary least squares regression lines. In water, at one meter the equivalent peak SPL of *Micronecta scholtzi* would be approximately 126 dB re 1 μ Pa. With a potential dipole gain of between 39-45 dB from the near field coupling to the bubble in order to reach the extreme amplitude recorded by *Micronecta scholtzi* a simple dipole source of 50 μm radius would have to be capable of generating an SPL of 80-85 dB (re 1 μPa) at 1 m, placing it comfortably within the regression lines for body size and peak SPL for other striating insects [2].

Micronecta scholtzi, in common with other Hydrocorisae, would be expected to be a polikothermic creature with the stroke speed of the plectrum and resultant frequency being dependent on temperature. Maximum pressure amplitudes will naturally occur when the click frequency of the plectrum on the *pars stridens* is matched to the 10 kHz Minnaert resonance of the air cushion, raising the question of whether *Micronecta scholtzi* uses a similar escapement mecha-

nism to regulate stroke speed as male crickets (the 'clockwork cricket') [18]. Here it is unclear that there is any selection advantage to louder calls and the resonator is still well, although not optimally, stimulated by the sawtooth waveform at 5 kHz. In addition the resonance frequency of the air cushion in Hydrocorisae changes with diving time as the oxygen is depleted, varying as much as 1 kHz between surfacings [10], again suggesting the loud call volume is an unintended by-product of the system and not something which contains useful information to a mate.
Near field acoustic coupling of bubble to source allows the transfer of energy from a high input efficiency, but low radiative efficiency source to a low-input efficiency and high radiative efficiency source. The system has potential applications in very low frequency underwater transducers, where energy losses from existing systems are extremely high [19, 20] due to the requirement that they work around their fundamental resonance frequency in order to generate enough acoustic power. For transducers working below 500 Hz this can make the working area necessarily large, requiring high electrical and mechanical excitation levels which consequent problems of piezoelectric efficiency (in the case of piezoelectric transducers) and mechanical fatigue. In separating the acoustic radiator (the bubble) from the source a much smaller and more electrically efficient piezoelectric source can drive a flexural bubble through near-field coupling and maintain the desirable radiation characteristics of a surface in volume pulsation.

Data accessibility

All data created during this research are openly available from the University of Strathclyde Pure/KnowledgeBase at http://dx.doi.org/10.15129/46c7cb9b-7966-40fa-947f-b9f65757f6a5

Competing interests

We have no competing interests.

Authors' contributions

AR carried out the mathematical analysis, carried out the finite element analysis, participated in the design of the study and drafted the manuscript; DH helped carry out the mathematical analysis, helped the conception of the study, and helped design the study; DM carried out the x-ray scans; JCJ helped carry out the mathematical analysis, and helped draft the manuscript; JFCW conceived of the study, designed the study, coordinated the study and helped draft the manuscript. All authors gave final approval for publication.

Acknowledgements

We acknowledge the assistance of Dr Jérôme Sueur of Muséum national d'Histoire naturelle, Département Systématique et Evolution, Paris, France.

Funding

Research at the University of Strathclyde leading to these results received funding from the European Research Council under the European Union's Seventh Framework Programme FP/2007-2013 / ERC Grant Agreement n. 615030.

Appendix - Derivation of bubble gains

The velocity potentials from the source and bubble evaluated at the bubble boundaries are related by:

$$\Phi_b^B = \Phi_s^B \left[\frac{\omega_0^2}{\omega^2} - 1 - \imath\delta\right]^{-1} \tag{5}$$

where the term ω_0 is the Minnaert resonance frequency of the bubble while δ is a damping parameter which encompasses radiative, thermal and viscous losses and $\imath$ is the imaginary unit. To illustrate the response of a bubble in the near-field of a source we consider the sound field from a simple monopole and dipole source. For a monopole source a standard pressure solution to the Helmholtz equation using the spherical harmonics functions in the near field would be:

$$\hat{p}_s^P(r,\omega) = \rho c \hat{v}_n^S \left(\frac{kr}{kr+\imath}\right)\frac{r_0}{r}e^{\imath k(r-r_s)} \tag{6}$$

where the position at point 'P' is reduced to the radial distance r, as the field should not change with spherical co-ordinates θ and ϕ. The remaining terms are the wavenumber $k = \omega c$, where c is the phase velocity of the wave and $\hat{v}_n^S$ is the time averaged normal velocity of the boundaries of the source. The bubble's operation as a monopole source can be described in the same form as equation 2. From the diagram in figure 1 the field at the bubble's boundaries can then be evaluated. Here we have assumed the bubble's radius to be sufficiently small in comparison to the wavelength that the pressure from the source will be uniform around the bubble boundaries, and take the field at distance d from the source:

$$\hat{p}_s^B(d,\omega) = \rho c \hat{v}_n^S \left(\frac{kr_s}{kr_s+\imath}\frac{r_s}{d}\right)e^{\imath k(d-r_s)} \tag{7}$$

$$\hat{p}_b^B(r_b;\omega) = \rho c \hat{v}_n^B \left(\frac{kr_b}{kr_b+\imath}\right). \tag{8}$$

Combining with the equation 1 above and taking $p = -\rho\frac{\partial\Phi}{\partial t} = \imath\omega\rho\Phi$ gives:

$$\imath\omega\rho^2 c\hat{v}_n^S \left(\frac{kr_s}{kr_s+\imath}\right)\frac{r_s}{d}e^{\imath k(d-r_s)} = \frac{\imath\omega\rho^2 c\hat{v}_n^B\left(\frac{kr_b}{kr_b+\imath}\right)}{\frac{\omega_0^2}{\omega^2} - 1 - \imath\delta} \tag{9}$$

this equation can be solved for the normal velocity of the bubble ($\hat{v}_n^B$) in terms of the source normal velocity, radius, separation distance, and the relative frequency to the Minnaert resonance:

$$\hat{v}_n^B = \hat{v}_n^S \frac{\frac{kr_s}{kr_s+\imath}\frac{r_s}{d}}{\frac{kr_b}{kr_b+\imath}\left(\frac{\omega_0^2}{\omega^2} - 1 - \imath\delta\right)}. \tag{10}$$

Similarly we can evaluate the pressure at point P in from the bubble and the source and describe the pressure gain from the bubble in the ratio $A = \frac{\hat{p}_b^P}{\hat{p}_s^P}$:

$$\hat{p}_s^P(r_1,\omega) = \rho c \hat{v}_n^S \left(\frac{kr_s}{kr_s+\imath}\right)\frac{r_s}{r_1}e^{\imath k(r_1-r_s)} \tag{11}$$

$$\hat{p}_s^B(r_2,\omega) = \rho c \hat{v}_n^B \left(\frac{kr_b}{kr_b+\imath}\right)\frac{r_b}{r_2}e^{\imath k(r_2-r_b)} \tag{12}$$

$$A = \frac{\frac{r_1 r_b}{dr_2}}{\frac{\omega_0^2}{\omega^2} - 1 - \imath\delta}e^{\imath k(r_2-r_1-r_b+d)} \tag{13}$$

For a point P in the far field the distances r_1 and r_2 can be approximated as equal leaving a simplified resonant expression for the gain which depends on the bubble radius and is inversely proportional to the separation between bubble and source.

$$A_{dB} = 20\log_{10}\left|\frac{\frac{r_b}{d}}{\frac{\omega_0^2}{\omega^2} - 1 - \imath\delta}\right|. \tag{14}$$

Similarly for a dipole source a standard solution for the pressure in the near field would be:

$$\hat{p}_s^P(r,\theta,\omega) = \rho c \hat{v}_z^S \left(\frac{kr_s(kr+\imath)}{k^2r_s^2 - 2 + \imath 2kr_s}\right)\left(\frac{r_s}{rd}\right)^2 \cos\theta e^{\imath k(r-r_s)} \tag{15}$$

where the velocity term $\hat{v}_z^S$ refers to the dipole movement of the source along the z-axis and θ is the angle between source and listening point. Using the same approach as before, evaluating the field at the bubble boundaries and substituting in equation 2:

$$\hat{p}_s^B(r,\theta_b,\omega) = \rho c \hat{v}_z^B \left(\frac{kr_s(kr+\imath)}{k^2r_s^2 - 2 + \imath 2kr_s}\right)\left(\frac{r_s}{rd}\right)^2 \cos\theta_b e^{\imath k(d-r_s)} \tag{16}$$

$$\hat{p}_b^B(r,\theta,\omega) = \rho c \hat{v}_n^B \left(\frac{kr_b}{kr_b+\imath}\right). \tag{17}$$

$$\rho c \hat{v}_n^B \left(\frac{kr_b}{kr_b+\imath}\right) = \rho c \hat{v}_z^B \left(\frac{kr_s(kr+\imath)}{k^2r_s^2 - 2 + \imath 2kr_s}\right)\left(\frac{r_s}{rd}\right)^2 \cos\theta_b \frac{e^{\imath k(d-r_s)}}{\frac{\omega_0^2}{\omega^2} - 1 - \imath\delta} \tag{18}$$

$$\hat{v}_n^B = \frac{\hat{v}_z^S(kr_b+\imath)}{kr_b}\frac{kr_b(kd+\imath)}{k^2r_s^2 - 2 + \imath 2kr_s}\left(\frac{r_s}{d}\right)^2 \cos\theta_b e^{\imath k(d-r_s)} \tag{19}$$

Evaluating the field at point P:

$$\hat{p}_s^P(r_1,\theta_1,\omega) = \rho c \hat{v}_z^S \frac{kr_s(kr_1+\imath)}{k^2r_s^2 - 2 + \imath 2kr_s}\left(\frac{r_s}{r_1}\right)^2 \cos\theta_1 e^{\imath k(r_1-r_2)} \tag{20}$$

$$\hat{p}_b^P(r_2,\theta_2,\omega) = \rho c \hat{v}_n^B \frac{kr_b}{kr_b+\imath}\frac{r_b}{r_2} e^{\imath k(r_2-r_b)} \tag{21}$$

$$A = \frac{\hat{p}_b^P}{\hat{p}_s^P} = \frac{\frac{kd+\imath}{d^2}\cos\theta_b \frac{r_b}{r}}{\frac{kr+\imath}{r^2}\cos\theta_1 \frac{\omega_0^2}{\omega^2} - 1 - \imath\delta} \tag{22}$$

$$A_{dB,dipole} = 20\log_{10}\left|\frac{\frac{kd+\imath}{d^2}\cos(\theta_b)\frac{r_b}{r}}{\frac{kr+\imath}{r^2}\cos(\theta_1)\left(\frac{\omega_0^2}{\omega^2} - 1 - \imath\delta\right)}\right| \tag{23}$$

References

[1] M. Parsons, "Respiratory significance of the thoracic and abdominal morphology of the three aquatic bugs ambrysus, notonecta and hesperocorixa (insecta, heteroptera)," *Zoomorphology*, vol. 66, no. 3, pp. 242–298, 1970.

[2] J. Sueur, D. Mackie, and J. F. Windmill, "So small, so loud: Extremely high sound pressure level from a pygmy aquatic insect (corixidae, micronectinae)," *PloS one*, vol. 6, no. 6, p. e21089, 2011.

[3] H. Bennet-Clark, "Size and scale effects as constraints in insect sound communication," *Philosophical Transactions of the Royal Society of London B: Biological Sciences*, vol. 353, no. 1367, pp. 407–419, 1998.

[4] A. Jansson, "Stridulation and its significance in the genus cenocorixa (hemiptera, corixidae)," *Behaviour*, vol. 46, no. 1, pp. 1–36, 1973.

[5] I. M. King, "Underwater sound production in micronecta batilla hale (heteroptera: Corixidae).," *Austral Entomology*, vol. 15, no. 1, pp. 35–43, 1976.

[6] W. J. Bailey, "Sound production in micronecta batilla hale (hemiptera: Corixidae) - an alternative structure," *Austral Entomology*, vol. 22, no. 1, pp. 35–38, 1983.

[7] A. Jansson, "Stridulation of micronectinae (heteroptera, corixidae)," in *Annales Entomologici Fennici*, vol. 55, pp. 161–175, Entomological Society Finland c/o Zoological Museum P Rautatiekatu 13, SF-0100 Helsinki, Finland, 1989.

[8] I. King, "Acoustic communication and mating behaviour in water bugs of the genus micronecta," *Bioacoustics*, vol. 10, no. 2-3, pp. 115–130, 1999.

[9] R. D. Alexander, "Acoustical communication in arthropods," *Annual review of entomology*, vol. 12, no. 1, pp. 495–526, 1967.

[10] J. Theiß, "Generation and radiation of sound by stribulating water insects as exemplified by the corixids," *Behavioral Ecology and Sociobiology*, vol. 10, no. 3, pp. 225–235, 1982.

[11] R. S. Seymour and P. G. Matthews, "Physical gills in diving insects and spiders: theory and experiment," *Journal of Experimental Biology*, vol. 216, no. 2, pp. 164–170, 2013.

[12] M. Devaud, T. Hocquet, J.-C. Bacri, and V. Leroy, "The minnaert bubble: an acoustic approach," *European Journal of Physics*, vol. 29, no. 6, p. 1263, 2008.

[13] G. Houghton, "The behaviour of particles in a sinusoidal velocity field," in *Proceedings of the Royal Society of London A: Mathematical, Physical and Engineering Sciences*, vol. 272, pp. 33–43, The Royal Society, 1963.

[14] M. Strasberg, "Gas bubbles as sources of sound in liquids," *The Journal of the Acoustical Society of America*, vol. 28, no. 1, pp. 20–26, 1956.

[15] M. Strasberg, "The pulsation frequency of nonspherical gas bubbles in liquids," *The Journal of the Acoustical Society of America*, vol. 25, no. 3, pp. 536–537, 1953.

[16] J. F. Williams and W. Hunter, "The scattering of multipole near-field sound by a gas bubble," in *Proceedings of the Royal Society of London A: Mathematical, Physical and Engineering Sciences*, vol. 314, pp. 363–385, The Royal Society, 1970.

[17] C. Girard and A. Dereux, "Near-field optics theories," *Reports on Progress in Physics*, vol. 59, no. 5, p. 657, 1996.

[18] H. Bennet-Clark and W. J. Bailey, "Ticking of the clockwork cricket: the role of the escapement mechanism," *Journal of experimental Biology*, vol. 205, no. 5, pp. 613–625, 2002.

[19] J.-N. Decarpigny, B. Hamonic, and O. B. Wilson, "The design of low frequency underwater acoustic projectors: present status and future trends," *IEEE Journal of Oceanic Engineering*, vol. 16, no. 1, pp. 107–122, 1991.

[20] B. Dubus, P. Mosbah, J.-R. Hartmann, and J. Garcin, "Ultra-low frequency underwater acoustic projectors: Present status and future trends," in *Proceedings of Meetings on Acoustics ICA2013*, vol. 19, p. 030020, ASA, 2013.